Accuracy improvement quantification using phase-separated PIV Measurements

F. Gökhan Ergin[1] *

1: CTA and Microfluidics Product Manager, Dantec Dynamics, DENMARK

Keywords: Particle Image Velocimetry, Two-Phase Flow, PIV measurement accuracy, Phase-separated PIV

ABSTRACT

This paper aims to quantify the Particle Image Velocimetry (PIV) measurement accuracy improvement along the phase boundaries of two-phase flows, due to the use of phase-separated PIV analysis, compared to conventional PIV analysis without separating the phases. To compute the true error produced by the PIV analysis, a patchwork of synthetic image pair with a known displacement is used as ground truth. As real flows might have arbitrary flow direction and magnitude across the phase boundary, the patchwork of image-pair includes a variety of direction combinations, i.e. flows running into each other or away from one another, shear flow, sink flow, flow towards a wall and flow away from a wall, flow running into a stagnant phase, flows with perpendicular directions, and flows that are 45° to each other. The relative error distribution along the boundaries reveals that the relative error level depends on the flow direction on each side of the boundary. Results indicate that using phase-separated PIV analysis can bring the measurement error level from ~200% down to ~5% along the boundaries.

1. Introduction

Cross-correlation based Particle Image Velocimetry (PIV) measurement accuracy is lower along the phase boundaries of two-phase flows because the interrogation windows contain information from both phases. Different seeding density, background intensity, velocity magnitude and flow direction conditions often exist across the boundary (Fig. 1), and the PIV algorithm selects only the highest correlation peak. The highest correlation peak is either influenced by the wrong phase across the boundary, or the correctly calculated displacement is erroneously detected as an outlier at a later stage and is subsequently replaced. Phase-separated PIV measurements minimize this problem and increase accuracy along the boundary by treating each phase separately. This type of measurement requires for each time step; (i) accurate detection of the phase boundary in consecutive frames, (ii) generation of dynamic phase masks, (iii) an accurate PIV evaluation of each phase and (iv) recombination of the flow fields. [1]

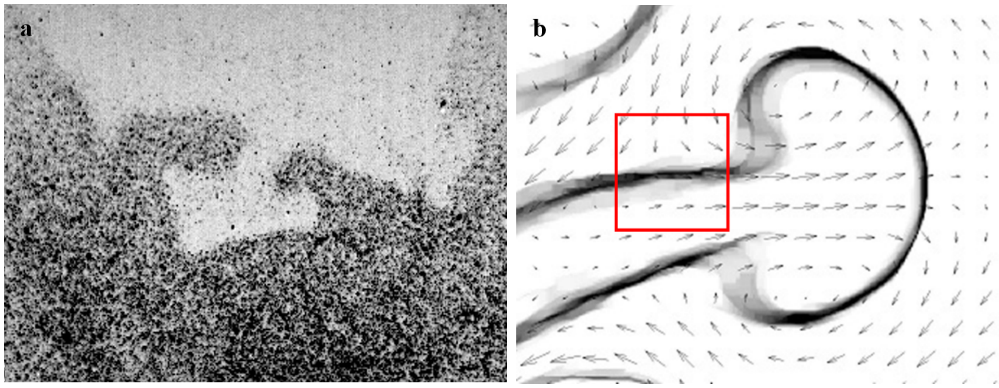

Fig. 1: (a) Different seeding conditions observed across the reaction zone in a combustion experiment. (b) Different flow conditions observed in the mixed-phase PIV results around a mushroom pattern in a magnetic micromixer. From Ref. [1].

A significant number of articles have been published in the literature taking advantage of the phase-separated PIV measurements [1]-[15] with the same goal; to improve the measurement accuracy along the dynamic phase boundaries. However, to the author's knowledge, none of these articles attempted to quantify the accuracy improvement, as this requires a known velocity field input on both sides of the interface. Because flow direction, flow speed, seeding and illumination conditions across the interface are random during an experiment, quantification of accuracy improvement is challenging simply using experimental data. For this reason, we use synthetic images for the quantification of the PIV accuracy improvement in two-phase flows.

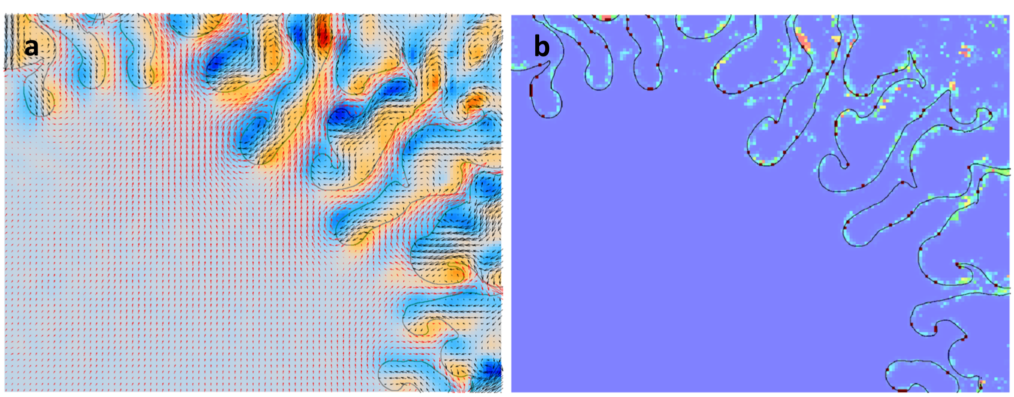

Fig. 2: (a) Phase-separated PIV measurements in a magnetic micromixer where colors indicate vorticity. (b) Magnitude of velocity difference between PIV results with and without phase separation shown with the phase boundary. From Ref. [15].

2. Method

It is clear from Ref. [1] that the phase-separated PIV measurements make a difference in the calculated velocity results along the boundary (Fig. 2). To call these differences actual accuracy improvements, a synthetic image pair with known displacement field must be used. In this section, we make a quantitative estimate of accuracy improvement as a result of phase separated PIV measurements using a 3-step procedure: First, a patchwork synthetic image with different flow directions and seeding densities is generated. Second, PIV analysis with and without phase separation is performed, and third, errors produced for each case with respect to the known displacement fields are compared.

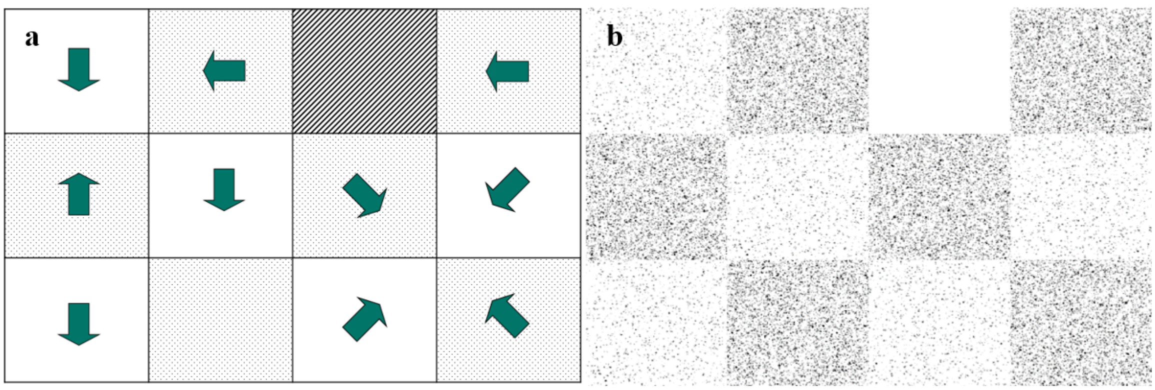

Fig. 3: (a) Possible flow and seeding scenarios across the boundary. (b) Synthetic image used for improvement estimation featuring different flow direction and seeding density configurations across phase boundaries (inverted).

The benefit of working with a patchwork image is to have a controlled input for the possible flow configurations across the boundary (Fig 3a). In this figure, several flow possibilities that can exist across a phase boundary are represented: These are; flows running into each other or away from one another (left column), shear flow (middle row, left 2 squares), sink flow (4 adjacent squares in lower right corner), flow towards a wall (top, right square) and flow away from a wall (top row 2nd square on the left), flow running into a stagnant phase (middle row 2nd square on the left), flows with perpendicular directions, and flows that are 45deg to each other. The patchwork image (Fig. 3b) is produced by stitching 256x256 pixel sub-images with different seeding densities. The seeding density of the densely seeded patches (0.042 particles/pixel) are three times that of the sparsely seeded patches (0.014 particles/pixel). On each square patch, two different known displacements are imposed: 5 pixels and 10 pixels, the latter value being typical for conventional planar PIV experiments.

3. Results

The PIV analysis is performed on individual sections and on the entire mixed-phase synthetic image pair using identical settings: 32x32 pixel interrogation windows, 75% overlap, no window or filter functions, universal outlier detection with a minimum normalization level of 0.1 and an acceptance limit of 2.0. The phase separated PIV measurements produce a displacement field very close to the input displacement field (Fig. 4a) and therefore not shown in a separate figure.

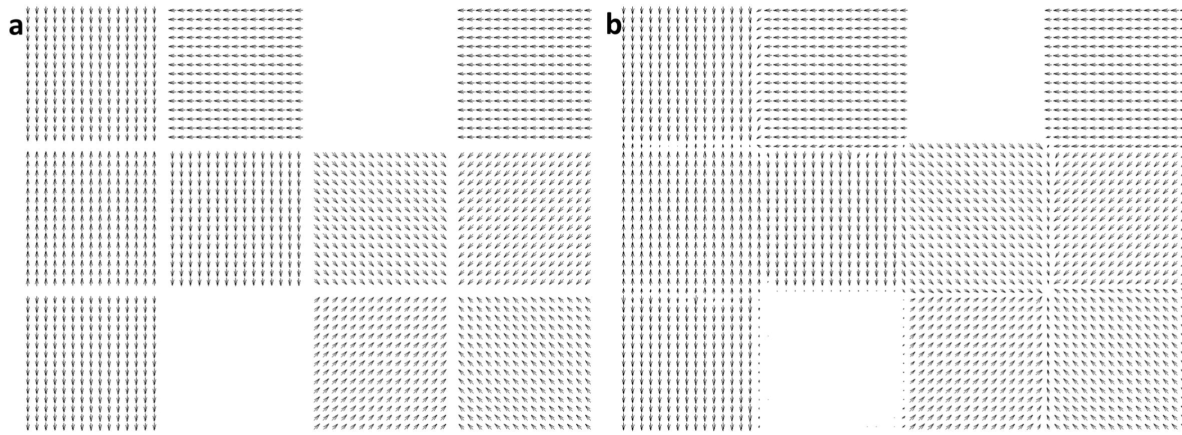

Fig. 4: (a) Velocity distribution of the known 5-pixel displacement field. (Ground truth) Distribution is similar to this with phase separation. (b) Velocity distribution of the same without phase separation (mixed-phase PIV). Every second vector is displayed.

The performance of each PIV result (with and without phase separation) can be compared by computing the deviation from the known displacement field (ground truth). The relative error is defined as the ratio of the deviation from the known displacement, and the magnitude of the known displacement. The spatial distribution of the relative error for the 5-pixel displacement is given in (Fig. 5):

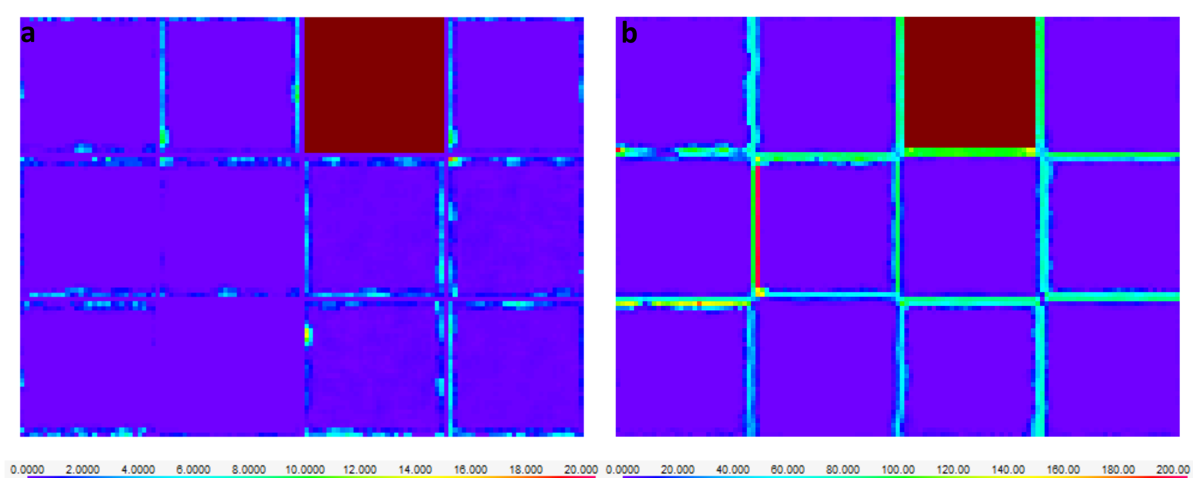

Fig. 5: Relative error distribution [in %] with respect to the known (5-pixel) displacement field. (a) With phase separation. (b) Without phase separation. The error range on the left is 10 times smaller than the one on the right.

As expected, the errors are located along the phase boundaries both for the phase-separated (Fig. 5a) and for the mixed-phase (Fig. 5b) PIV analysis. For the 5-pixel displacement case, while the relative error along the phase boundaries can be as high as ~200% for the mixed phase analysis, it is on the order of 1-5% using phase separation. The ~200% error is only observed along the boundary for the shear flow region (between the left 2 squares in the middle row) and is consistent with the expectations: In the shear flow region, the densely seeded flow on the left going upwards dominates and overrides the sparsely seeded flow on the right going downwards. The result is a velocity estimate with equal magnitude but opposite direction (~200% error). Similarly, ~100% error is observed around the square without seeding, which represents a bubble (Fig. 5b brown patch on the top row). On the other hand, the 1-5% relative error level observed along the phase boundaries for the case with phase separation can be explained by in-plane loss-of-pairs [16]. Far away from the boundaries, the relative error is ≤ 1%. This is also expected because the accuracy of this PIV algorithm is reported as 0.055 pixels [17]. The general findings are quite similar for the 10-pixel displacement case.

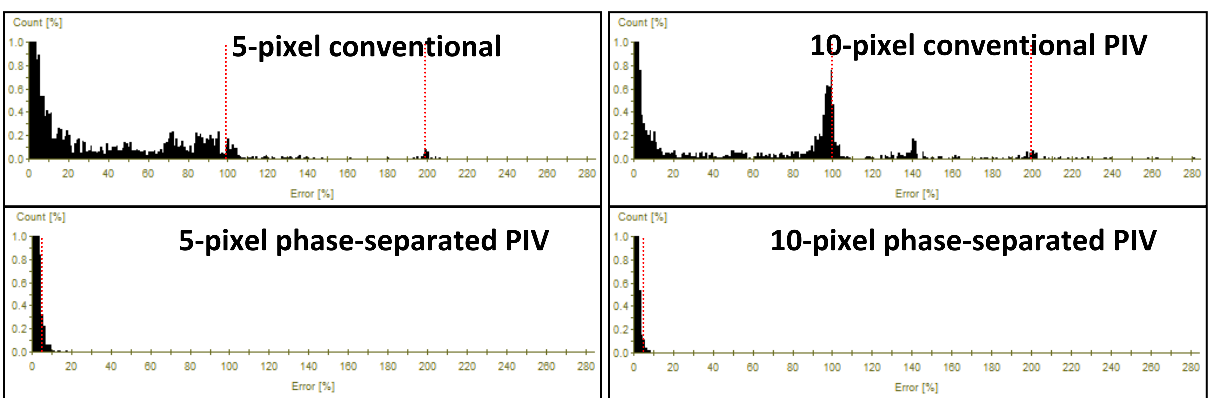

Fig. 6 Relative error histograms with respect to the ground truth. Left: 5-pixel displacement. Right: 10-pixel displacement. Top: Without phase separation. Bottom: With phase separation. Dashed red lines mark the 5%, 100% and 200% error values.

The impact of phase separated PIV analysis is more apparent when the relative error histograms of phase separated and mixed-phase PIV results are compared (Fig. 6). In this figure, the error histograms on the top belong to results without phase separation and the histograms on the bottom are the error produced with phase separation. The error histograms on the left are produced with 5-pixel displacement, and the ones on the right are produced with 10-pixel displacement. The vertical range in the histograms are all set to 0-1% of the count in order to focus on the details for the vectors close to the phase boundaries. (Counts >1% are not shown in Fig. 6 for clarity). The horizontal ranges in histograms are all set to a common value to make a direct visual comparison on the error reduction.

4. Conclusions

Quantification of accuracy improvement using phase-separated PIV analysis is presented. It was always suggested that phase-separated PIV analysis should improve PIV accuracy along phase boundaries. With the results presented in this work, we can see that in certain scenarios, phase separated PIV measurements can bring the relative error level from ~200% down to ~5% along phase boundaries, which is a significant improvement. It was also observed that the error magnitude strongly depends on the flow direction on each side of the boundary. For example, the ~200% error is only seen with the shear flow case. In real experiments, it is also expected that very thin boundary layers are present along the phase boundaries, where sharp velocity gradients exist. In these regions, the ~5% error levels along the phase boundaries can be further improved using interrogation window masking [18], [19]; vector replacement techniques [20] or ultimately by using Particle Tracking Velocimetry [21].

5. Acknowledgements

The author wishes to thank Mads Bering Andersen in the "image stitching" algorithm development for the generation of the synthetic image patch in Fig. 3b.

6. References

[1] F. G. Ergin, J. Olofsson, P. Petersson, and N. F. Gade-Nielsen, "A hybrid phase boundary detection technique for two-phase-flow PIV measurements," *Flow Meas. Instrum.*, vol. 74, p. 101776, Aug. 2020, doi: 10.1016/j.flowmeasinst.2020.101776.

[2] L. Gui and W. Merzkirch, "Phase-Separation of Piv Measurements in Two-Phase Flow By Applying a Digital Mask Technique," in *EERCOFTAC Bulletin*, 1996, vol. 30, pp. 45–48.

[3] R. Lindken, L. Gui, and W. Merzkirch, "Velocity Measurements in Multiphase Flow by Means of Particle Image Velocimetry," *Chem. Eng. Technol.*, vol. 22, no. 3, pp. 202–206, Mar. 1999, doi: 10.1002/(SICI)1521-4125(199903)22:3<202::AID-CEAT202>3.0.CO;2-K.

[4] A. Sanchis and A. Jensen, "Dynamic masking of PIV images using the Radon transform in free surface flows," *Exp. Fluids*, vol. 51, no. 4, pp. 871–880, Oct. 2011, doi: 10.1007/s00348-011-1101-7.

[5] O. Carrier, F. G. Ergin, H. Z. Li, B. B. Watz, and D. Funfschilling, "Time-resolved mixing and flow-field measurements during droplet formation in a flow-focusing junction," *J. Micromechanics Microengineering*, vol. 25, no. 8, p. 84014, 2015, doi: 10.1088/0960-1317/25/8/084014.

[6] K. T. Kiger and C. Pan, "PIV Technique for the Simultaneous Measurement of Dilute Two-Phase Flows," *J. Fluids Eng.*, vol. 122, no. 4, p. 811, 2000, doi: 10.1115/1.1314864.

[7] R. Lindken and W. Merzkirch, "Velocity measurements of liquid and gaseous phase for a system of bubbles rising in water," *Exp. Fluids*, vol. 29, no. 7, pp. S194–S201, Dec. 2000, doi: 10.1007/s003480070021.

[8] R. Lindken and W. Merzkirch, "A novel PIV technique for measurements in multiphase flows and its application to two-phase bubbly flows," *Exp. Fluids*, vol. 33, no. 6, pp. 814–825, Dec. 2002, doi: 10.1007/s00348-002-0500-1.

[9] N. G. Deen, J. Westerweel, and E. Delnoij, "Two-phase PIV in bubbly flows: Status and trends," *Chem. Eng. Technol.*, vol. 25, no. 1, pp. 97–101, 2002, doi: 10.1002/1521-

4125(200201)25:1<97::AID-CEAT97>3.0.CO;2-7.

[10] D. A. Khalitov and E. K. Longmire, "Simultaneous two-phase PIV by two-parameter phase discrimination," *Exp. Fluids*, vol. 32, no. 2, pp. 252–268, 2002, doi: 10.1007/s003480100356.

[11] K. D. Driscoll, V. Sick, and C. Gray, "Simultaneous air/fuel-phase PIV measurements in a dense fuel spray," *Exp. Fluids*, vol. 35, no. 1, pp. 112–115, 2003, doi: 10.1007/s00348-003-0647-4.

[12] M. L. Riethmuller, A. M. F. R. Pinto, S. Nogueira, J. B. L. M. Campos, and R. G. Sousa, "Simultaneous PIV and pulsed shadow technique in slug flow: a solution for optical problems," *Exp. Fluids*, vol. 35, no. 6, pp. 598–609, 2003, doi: 10.1007/s00348-003-0708-8.

[13] M. J. Sathe, I. H. Thaker, T. E. Strand, and J. B. Joshi, "Advanced PIV/LIF and shadowgraphy system to visualize flow structure in two-phase bubbly flows," *Chem. Eng. Sci.*, vol. 65, no. 8, pp. 2431–2442, Apr. 2010, doi: 10.1016/j.ces.2009.11.014.

[14] F. G. Ergin, "Dynamic masking techniques for Particle Image Velocimetry," *Isi Bilim. Ve Tek. Dergisi/ J. Therm. Sci. Technol.*, vol. 37, no. 2, pp. 61–74, 2017.

[15] F. G. Ergin, J. Olofsson, and N. F. Gade-nielsen, "Phase Separated PIV Measurements Using Phase Boundary Detection," 2017.

[16] S. Scharnowski and C. J. Kähler, "On the loss-of-correlation due to PIV image noise," *Exp. Fluids*, vol. 57, no. 7, p. 119, Jul. 2016, doi: 10.1007/s00348-016-2203-z.

[17] F. G. Ergin, B. B. Watz, K. Erglis, and A. Cēbers, "Time-resolved velocity measurements in a magnetic micromixer," *Exp. Therm. Fluid Sci.*, vol. 67, pp. 6–13, 2015, doi: 10.1016/j.expthermflusci.2015.02.019.

[18] F. G. Ergin, "PIV accuracy improvement near stationary walls using interrogation window masking," 2017.

[19] F. G. Ergin, "An automatic static masking technique using Particle Image Velocimetry image ensembles," *Exp. Therm. Fluid Sci.*, vol. 128, p. 110431, Oct. 2021, doi: 10.1016/j.expthermflusci.2021.110431.

[20] R. Theunissen, F. Scarano, and M. L. Riethmuller, "On improvement of PIV image interrogation near stationary interfaces," *Exp. Fluids*, vol. 45, no. 4, pp. 557–572, Oct. 2008, doi: 10.1007/s00348-008-0481-9.

[21] C. J. Kähler, S. Scharnowski, and C. Cierpka, "On the uncertainty of digital PIV and PTV near walls," *Exp. Fluids*, vol. 52, no. 6, pp. 1641–1656, 2012, doi: 10.1007/s00348-012-1307-3.